LA-UR-00-3332

Title: INTEGRATING LINEAR INTERPOLATION FUNCTIONS ACROSS TRIANGULAR AND TETRAHEDRAL CELL BOUNDARIES

Author(s) Jerry S. Brock, Los Alamos National Laboratory
J. Renae Wiseman, U. S. Air Force Academy

Submitted to: Conference on Computational Physics 2000
Gold Coast, Queensland, Australia, December 3–8, 2000

Photograph by Chris J. Lindberg

Los Alamos
NATIONAL LABORATORY

Form 836 (10/96)

December 2000 LA-UR-00-3332

Integrating Linear Interpolation Functions Across Triangular and Tetrahedral Cell Boundaries

Jerry S. Brock, Applied Physics Division
Los Alamos National Laboratory, Los Alamos, NM 87545

J. Renae Wiseman, Mathematics Department
U. S. Air Force Academy, Colorado Springs, CO 80841

Abstract

Computational models of particle dynamics often exchange solution data with discretized continuum-fields using interpolation functions. These particle methods require a series expansion of the interpolation function for two purposes: numerical analysis used to establish the model's consistency and accuracy, and logical-coordinate evaluation used to locate particles within a grid. This report presents *discrete-expansions* for two linear interpolation functions commonly used within triangular and tetrahedral cell geometries. Discrete-expansions, which are similar to a multi-variable Taylor's series, account for interpolation discontinuities across cell boundaries and are, therefore, valid throughout a discretized domain. Application of linear discrete-expansions for numerical analysis and localization within particle methods is outlined and discussed. Verification of linear discrete-expansions is demonstrated on a simple test problem.

LA-UR-00-3332

Integrating Linear Interpolation Functions Across Triangular and Tetrahedral Cell Boundaries

Introduction

Particle methods, computational models of particle dynamics, are often solved concurrently with discretized continuum-field equations. Interactive particle methods, including models of liquid sprays, bubble dynamics, and material-interface tracking, strongly couple the governing equations through the bilateral exchange of mass, momentum, and energy. In contrast, reactive particle methods, including models of atmospheric transport, porous-media diffusion, and transient mixing, weakly couple the governing equations; reactive particles simply respond to the entraining continuum field. Another reactive method, used extensively for solution visualization, free-surface tracking, and front tracking, is the tracer-particle method which advects a massless particle with an interpolated velocity. Both interactive and reactive particle methods exchange data with discrete fields using interpolation functions. The focus of this research was on the role of two linear interpolation functions commonly used within particle methods.

Particle methods often use interpolation functions directly to evaluate terms in their governing equations. A Taylor's series of the interpolation function, expanded from the particle's cell, is required to perform analytical studies of these numerical methods. The numerical analyses include establishing the model's mathematical consistency and numerical accuracy. The particle's equations, including kinematic equations-of-motion, are often numerically integrated using multi-step methods such as Runge-Kutta methods. The interpolated quantities within the particle's discretized governing equations may be evaluated in a neighboring cell, and the required interpolation expansion would then extend through multiple cells in the grid. Derivatives of interpolation functions, however, are generally not continuous across cell boundaries and, therefore, a Taylor's series is not valid in this situation. An alternative expansion for linear interpolation functions is required to complete numerical analyses for these particle methods.

Particle methods also often use interpolation functions indirectly to evaluate particle-grid connectivity data: the identity of the grid cell in which the particle resides and the particle's logical-coordinate position vector relative to that cell. Particle localization establishes this data using cell-searching and logical-coordinate evaluation methods [1-7]. Cell-searching methods typically use the particle's logical coordinates to both direct and halt the search. Logical-coordinate evaluation involves transforming a physical-space position vector into a local coordinate system, and, as described below, existing methods are based on interpolation expansions. Particle methods, therefore, require interpolation expansions for numerical analysis and localization, and the mathematical expression required for both purposes is identical.

While multi-cell Taylor's series of interpolation functions are generally not valid for numerical analyses, modified versions of these expansions are used for particle localization. For spatial-transformation, the arguments of the interpolation function are logical-coordinate and cell-vertex coordinate vectors. Existing logical-coordinate evaluation methods, generalized in Reference [1] for various cell geometries, were developed from a truncated, single-variable Taylor's series expansion of the interpolation function [1,3,5-7]. The modified Taylor's series avoids discontinuous interpolation derivatives across cell boundaries by ignoring the function's dependence on cell-vertex coordinates. Furthermore, non-linear spatial-transformation problems are linearized by only considering the interpolation function's first-order dependence on logical coordinates. The iterative solution of the resulting system of equations is, however, neither algorithmically robust nor computationally efficient. An alternative expansion for linear interpolation functions is required for robust and efficient particle localization methods.

An alternative type of expansion, a *discrete-expansion*, was recently proposed and validated for multi-linear interpolation functions [8-12]. Discrete-expansions are similar to multi-variable expansions but, unlike a Taylor's series, they are valid throughout a discretized domain. Discrete-expansions are valid for numerical analyses since they acknowledge the full functional dependence of interpolation and account for discontinuous derivatives across cell boundaries. Furthermore, the solution of discrete-expansions for logical-coordinate evaluation is both algorithmically robust and computationally efficient. Using a simple finite-difference technique, a single discrete-expansion was developed for trilinear interpolation defined within three-dimensional hexahedral cells [8,9]. Multiple discrete-expansions were recently developed for linear and bilinear interpolation functions defined within triangular [10,11] and quadrilateral cells [10,12]. These two-dimensional expansions were developed using a total-differential technique.

This report presents the development of discrete-expansions for linear interpolation defined within three-dimensional tetrahedral cell geometries. This report is will also show that these new discrete-expansions are identical to those for triangular cells; linear interpolation in two-dimensions is a subset of the three-dimensional problem. The development effort and discussion will, therefore, focus on three-dimensional linear interpolation. Finally, the unique formulations and characteristics of discrete-expansions for linear interpolation will also be identified. This report continues by parametrically integrating the linear interpolation function's total-differential between two particles located in separate, non-contiguous grid cells. Application of the new interpolation expansions for numerical analysis or localization within particle methods is beyond the scope of this report. The utility of linear discrete-expansions for these purposes, however, is outlined and discussed, and a summary concludes this report. An appendix then presents a test problem, which clearly demonstrates the new discrete-expansions validity.

Linear Interpolation

Three-dimensional computational space is frequently discretized into tetrahedral cells, particularly around complex geometries. Linear functions are often applied within these cells for data interpolation and spatial-transformation. Interpolation produces a continuous mapping of discrete data, often located at cell-vertices, to any position within the cell. Spatial transformation includes mapping cell geometries from a physical-space, $\bar{X} = (x, y, z)^T$, to a logical-space, $\bar{\xi} = (\xi, \eta, \zeta)^T$, coordinate system; see Figure 1. The linear function is dependent upon both $\bar{\xi}$ and the cell-vertex (cv) coordinate vector, $\bar{X}^{cv} = ({}^0\bar{X}, {}^1\bar{X}, {}^2\bar{X}, {}^3\bar{X})^T$, as presented in Equation 1.

$$\begin{aligned} \bar{X}(\bar{\xi}, \bar{X}^{cv}) = {} & (1 - \xi - \eta - \zeta) \, {}^0\bar{X} \\ & + (\quad \xi \quad) \, {}^1\bar{X} \\ & + (\quad \eta \quad) \, {}^2\bar{X} \\ & + (\quad \zeta \quad) \, {}^3\bar{X} \end{aligned} \tag{1}$$

Equation 1 is linear with respect to both the logical-coordinates, $\bar{\xi}$, and cell-vertex coordinates, $\bar{X}^{cv}$. While the physical coordinates of the tetrahedral's vertices are arbitrary, the transformed or logical-coordinates are bound by $\xi \geq 0$, $\eta \geq 0$, $\zeta \geq 0$, and $\xi + \eta + \zeta \leq 1$. Linear interpolation within two-dimensional triangular cell geometries may be obtained from Equation 1 by setting $\zeta = 0$. Similarly, linear interpolation within one-dimensional line-elements may be obtained from Equation 1 by setting $\eta = \zeta = 0$.

Total Differential

Using the interpolation function, $\bar{X}(\bar{\xi}, \bar{X}^{cv})$, the objective is to establish a relationship between the finite change of the physical coordinates, $\Delta\bar{X}$, the logical coordinates, $\Delta\bar{\xi}$, and the cell-vertex coordinates, $\Delta\bar{X}^{cv}$. The function's total-differential provides a relationship between infinitesimal changes of these coordinates, $d\bar{X} = f(d\bar{\xi}, d\bar{X}^{cv})$, as presented in Equation 2.

$$d\bar{X} = \frac{\partial \bar{X}(\bar{\xi}, \bar{X}^{cv})}{\partial \bar{\xi}} \, d\bar{\xi} + \frac{\partial \bar{X}(\bar{\xi}, \bar{X}^{cv})}{\partial \bar{X}^{cv}} \, d\bar{X}^{cv} \tag{2}$$

Integration of Equation 2 between two particle end-states will provide the relationship $\Delta\bar{X} = f(\Delta\bar{\xi}, \Delta\bar{X}^{cv})$, which functionally represents a discrete-expansion for interpolation.

Logical Coordinate Derivative

The linear interpolation function's total-differential includes two first-order derivatives or transformation matrices that are scaled by differential-coordinate vectors. The first derivative in

Equation 2 represents a coordinate-transformation or Jacobian matrix, $J = \partial\bar{X}/\partial\bar{\xi}$. The Jacobian matrix's square structure is defined in Equation 3 for a three-dimensional transformation.

$$\left[\frac{\partial\bar{X}}{\partial\bar{\xi}}\right]_{3x3} = \left[\frac{\partial\bar{X}}{\partial\xi}\ \frac{\partial\bar{X}}{\partial\eta}\ \frac{\partial\bar{X}}{\partial\zeta}\right]_{3x3} = \begin{bmatrix} \frac{\partial x}{\partial\xi} & \frac{\partial x}{\partial\eta} & \frac{\partial x}{\partial\zeta} \\ \frac{\partial y}{\partial\xi} & \frac{\partial y}{\partial\eta} & \frac{\partial y}{\partial\zeta} \\ \frac{\partial z}{\partial\xi} & \frac{\partial z}{\partial\eta} & \frac{\partial z}{\partial\zeta} \end{bmatrix}_{3x3} \tag{3}$$

The size of the Jacobian matrix is determined by the number of spatial dimensions. Elements of the coordinate-transformation matrix are most easily defined using column vectors. For three-dimensional linear interpolation, these derivatives are presented in Equation 4.

$$\begin{aligned} \frac{\partial\bar{X}}{\partial\xi}(\bar{X}^{cv}) &= {}^{1}\bar{X} - {}^{0}\bar{X} \\ \frac{\partial\bar{X}}{\partial\eta}(\bar{X}^{cv}) &= {}^{2}\bar{X} - {}^{0}\bar{X} \\ \frac{\partial\bar{X}}{\partial\zeta}(\bar{X}^{cv}) &= {}^{3}\bar{X} - {}^{0}\bar{X} \end{aligned} \tag{4}$$

Each derivative within Equation 4 is a linear function of the cell-vertex coordinates. The Jacobian matrix for three-dimensional linear interpolation, which combines these column vectors, is, therefore, a linear function with respect to $\bar{X}^{cv}$: $J = \partial\bar{X}(\bar{X}^{cv})/\partial\bar{\xi}$.

Cell-Vertex Coordinate Derivative

The second derivative in the linear interpolation function's total-differential, Equation 2, represents a geometry-transformation matrix. The matrix structure of $\partial\bar{X}/\partial\bar{X}^{cv}$, the cell-vertex coordinate derivative, is defined in Equation 5 for tetrahedral cell geometries.

$$\left[\frac{\partial\bar{X}}{\partial\bar{X}^{cv}}\right]_{3x12} = \left[\frac{\partial\bar{X}}{\partial^{0}\bar{X}}\ \frac{\partial\bar{X}}{\partial^{1}\bar{X}}\ \frac{\partial\bar{X}}{\partial^{2}\bar{X}}\ \frac{\partial\bar{X}}{\partial^{3}\bar{X}}\right]_{3x12} \tag{5}$$

The geometry-transformation matrix is non-square. The number of rows and columns in this matrix are determined by the problem dimension size and the number of elements within the cell-vertex coordinate vector, $\bar{X}^{cv}$. The size of $\bar{X}^{cv}$ is equal to the number of spatial dimensions multiplied by the number of cell vertices. As presented, the geometry-transformation matrix may

be partitioned into sub-matrices, each of which is associated with a single cell-vertex position. One sub-matrix, associated with any cell-vertex number ‘v’, is presented in Equation 6.

$$\left[\frac{\partial \bar{X}}{\partial^v \bar{X}}\right]_{3x3} = \left[\frac{\partial \bar{X}}{\partial^v x} \quad \frac{\partial \bar{X}}{\partial^v y} \quad \frac{\partial \bar{X}}{\partial^v z}\right]_{3x3} = \begin{bmatrix} \frac{\partial x}{\partial^v x} & \frac{\partial x}{\partial^v y} & \frac{\partial x}{\partial^v z} \\ \frac{\partial y}{\partial^v x} & \frac{\partial y}{\partial^v y} & \frac{\partial y}{\partial^v z} \\ \frac{\partial z}{\partial^v x} & \frac{\partial z}{\partial^v y} & \frac{\partial z}{\partial^v z} \end{bmatrix}_{3x3} \tag{6}$$

The square structure and size of each partition within the geometry-transformation matrix are similar to the Jacobian matrix, Equation 3. In contrast to the full Jacobian matrix, however, each of the sub-matrices within $\partial \bar{X} / \partial \bar{X}^{cv}$ are diagonal as presented in Equation 7.

$$\left[\frac{\partial \bar{X}}{\partial^v \bar{X}}\right]_{3x3} = \begin{bmatrix} \frac{\partial x}{\partial^v x} & 0 & 0 \\ 0 & \frac{\partial y}{\partial^v y} & 0 \\ 0 & 0 & \frac{\partial z}{\partial^v z} \end{bmatrix}_{3x3} \tag{7}$$

The non-zero elements of the sub-matrices within $\partial \bar{X} / \partial \bar{X}^{cv}$ are most easily defined for each cell-vertex position. These elements, $\partial x / \partial^v x$, $\partial y / \partial^v y$, and $\partial z / \partial^v z$, are the basis functions used within the three-dimensional linear interpolation function as presented in Equation 8.

$$\begin{aligned} \frac{\partial x}{\partial^0 x}(\bar{\xi}) &= \frac{\partial y}{\partial^0 y}(\bar{\xi}) = \frac{\partial z}{\partial^0 z}(\bar{\xi}) = (1 - \xi - \eta - \zeta) \\ \frac{\partial x}{\partial^1 x}(\bar{\xi}) &= \frac{\partial y}{\partial^1 y}(\bar{\xi}) = \frac{\partial z}{\partial^1 z}(\bar{\xi}) = (\xi) \\ \frac{\partial x}{\partial^2 x}(\bar{\xi}) &= \frac{\partial y}{\partial^2 y}(\bar{\xi}) = \frac{\partial z}{\partial^2 z}(\bar{\xi}) = (\eta) \\ \frac{\partial x}{\partial^3 x}(\bar{\xi}) &= \frac{\partial y}{\partial^3 y}(\bar{\xi}) = \frac{\partial z}{\partial^3 z}(\bar{\xi}) = (\zeta) \end{aligned} \tag{8}$$

For each cell-vertex, the non-zero derivatives are identical: $\partial x / \partial^v x = \partial y / \partial^v y = \partial z / \partial^v z$. Each sub-matrix may then be defined as an identity matrix scaled by an interpolation basis

function. The derivatives within Equation 8 are linear functions of the logical-coordinates. The geometry-transformation matrix for three-dimensional linear interpolation, which combines these column vectors, is, therefore, a linear function with respect to $\bar{\xi}$: $\partial\bar{X}(\bar{\xi})/\partial\bar{X}^{cv}$.

Since linear interpolation is linear with respect to both $\bar{\xi}$ and $\bar{X}^{cv}$, the transformation matrices, first-order derivatives, are functions of only one variable; the coordinate-transformation matrix is only a function of $\bar{X}^{cv}$ and the geometry-transformation matrix is only a function of $\bar{\xi}$. The linear interpolation function's simplified total-differential is presented in Equation 9.

$$d\bar{X} = \frac{\partial\bar{X}}{\partial\bar{\xi}}(\bar{X}^{cv})\, d\bar{\xi} + \frac{\partial\bar{X}}{\partial\bar{X}^{cv}}(\bar{\xi})\, d\bar{X}^{cv} \tag{9}$$

Integration Method

The objective is to integrate the linear function's total-differential, Equation 9, to obtain a discrete-expansion for interpolation: $\Delta\bar{X} = f(\Delta\bar{\xi}, \Delta\bar{X}^{cv})$. The integration limits are two particles located in separate grid cells: State 1, $\bar{X}_1 = \bar{X}(\bar{\xi}_1, \bar{X}_1^{cv})$, and State 2, $\bar{X}_2 = \bar{X}(\bar{\xi}_2, \bar{X}_2^{cv})$. The computational sub-domains in which the particles reside are not desired to be connected in physical-space. Integration of the total-differential is represented in Equation 10.

$$\int_1^2 d\bar{X} = \int_1^2 \frac{\partial\bar{X}}{\partial\bar{\xi}}(\bar{X}^{cv})\, d\bar{\xi} + \int_1^2 \frac{\partial\bar{X}}{\partial\bar{X}^{cv}}(\bar{\xi})\, d\bar{X}^{cv} \tag{10}$$

The linearity and continuity of the derivatives in the total-differential affect the integration process used to obtain a discrete-expansion. The linearity of the interpolation derivatives determines the complexity of the integration process. For linear interpolation, both the coordinate and geometry-transformation matrices are linear with respect to either $\bar{\xi}$ or $\bar{X}^{cv}$. More importantly, continuity of the interpolation derivatives is required for the total-differential to be valid within a specified region. Solution of Equation 10 in a single cell is straightforward; the interpolation derivatives are guaranteed to be continuous in this region. In contrast, if the limits of integration cross a cell boundary, solution of Equation 10 is more complex.

Solution of Equation 10 between particles located in separate but adjoining cells involves integrating the total-differential through two unique coordinate systems. While the form of the interpolation expression is identical for each cell, the two functions are different; they have distinct cell-vertex coordinate vectors. Along their common cell-edge, linear interpolation functions are continuous but their derivatives are generally discontinuous. Direct integration of the total-differential is, therefore, not possible along any pathline that crosses a cell boundary.

Discrete-expansions may be obtained from Equation 10 if the integration pathline is partitioned or if the integration coordinate-space is appropriately parameterized.

An integration pathline that passes between adjoining cells may be partitioned into two line-segments, each defined within a separate coordinate system. The integrals within Equation 10 are similarly partitioned into cell-based segments along which the interpolation derivatives are guaranteed to be continuous. Integration along this two-segment pathline would proceed within the first cell from State 1 to the common cell edge, then within the second cell to State 2. While this procedure represents a valid method of solution for Equation 10, it is algorithmically complex and computationally expensive. Furthermore, if the particle end-states are located within non-contiguous grid cells, this solution method is prohibitively complex and expensive.

Parameterization

Alternatively, the coordinate-space between the limits of integration can be parameterized. Parameterization removes the concept of multiple coordinate systems and, thus, discontinuous interpolation derivatives across cell boundaries, by creating a single coordinate-space between two particles. The integration end-states can then be defined within any two cells, including non-contiguous cells. While the form of the parameterization function is arbitrary, it must be differentiable; it is embedded within the parameterized interpolation function. Derivatives of the parameterized interpolation function are then guaranteed to be continuous. The parameterized total-differential, therefore, may be integrated without requiring a partitioned pathline.

To create a single coordinate-space between two particles, each of the physical, logical, and cell-vertex coordinates must be parameterized; particle states are a collection of these vectors. A simple linear technique using the variable ‘s’, where $0 \le s \le 1$, was selected in this research. The parameterized coordinates, $\overline{X}(s)$, $\overline{\xi}(s)$ and $\overline{X}^{cv}(s)$, then vary linearly along any integration pathline. Integration limits for the parameterized total-differential are the bounding limits of the variable ‘s’. Integration of the parameterized total-differential is represented in Equation 11.

$$\int_0^1 \frac{\partial \overline{X}(s)}{\partial s}\, ds = \int_0^1 \frac{\partial \overline{X}}{\partial \overline{\xi}}(\overline{X}^{cv}(s))\, \frac{\partial \overline{\xi}(s)}{\partial s}\, ds + \int_0^1 \frac{\partial \overline{X}}{\partial \overline{X}^{cv}}(\overline{\xi}(s))\, \frac{\partial \overline{X}^{cv}(s)}{\partial s}\, ds \qquad (11)$$

Solution of Equation 11 requires an integration pathline defined between the particle States 1 and 2. The only restriction on the limits of integration are that the end-state variables form a consistent set of coordinates as described by the interpolation function: $\overline{X} = \overline{X}(\overline{\xi}, \overline{X}^{cv})$. The integration pathline for the parameterized total-differential traverses through the $(\overline{\xi}, \overline{X}^{cv})$ plane since these vectors are the arguments of the spatial-transformation function. The

parameterization function, however, does not prescribe the shape of the integration pathline. Three pathlines, commonly used for parameterized integration problems, were selected by this research to solve Equation 11: direct, upper-step, and lower-step integration pathlines.

Direct Integration Pathline

The first integration pathline used to solve Equation 11 is a straight or direct line between particle States 1 and 2; see Figure 2. The parameterized coordinates, which reduce to the particle end-state coordinates at the bounding limits of integration, are presented in Equation 12.

$$\begin{aligned} \text{State 1} \rightarrow \text{State 2} \quad : \quad \overline{X}(s) &= (1-s)\,\overline{X}_1 + (s)\,\overline{X}_2 \\ \overline{\xi}(s) &= (1-s)\,\overline{\xi}_1 + (s)\,\overline{\xi}_2 \\ \overline{X}^{cv}(s) &= (1-s)\,\overline{X}_1^{cv} + (s)\,\overline{X}_2^{cv} \end{aligned} \tag{12}$$

Solution of Equation 11 along the direct integration pathline is represented in Equation 13, where the interpolation derivatives are appropriately labeled.

$$\begin{aligned} \int_0^1 \left.\frac{\partial \overline{X}(s)}{\partial s}\right|_{1\rightarrow 2} ds \;=\; & \int_0^1 \left.\frac{\partial \overline{X}}{\partial \overline{\xi}}(\overline{X}^{cv}(s))\right|_{1\rightarrow 2} \left.\frac{\partial \overline{\xi}(s)}{\partial s}\right|_{1\rightarrow 2} ds \\ & + \int_0^1 \left.\frac{\partial \overline{X}}{\partial \overline{X}^{cv}}(\overline{\xi}(s))\right|_{1\rightarrow 2} \left.\frac{\partial \overline{X}^{cv}(s)}{\partial s}\right|_{1\rightarrow 2} ds \end{aligned} \tag{13}$$

Since the parameterized coordinates are linear functions, their derivatives are constant finite-difference vectors: $\partial \overline{X}(s)/\partial s = \Delta \overline{X}$, $\partial \overline{\xi}(s)/\partial s = \Delta \overline{\xi}$, and $\partial \overline{X}^{cv}(s)/\partial s = \Delta \overline{X}^{cv}$. These difference vectors are defined between particle States 1 and 2: $\Delta \overline{X} = \overline{X}_2 - \overline{X}_1$, $\Delta \overline{\xi} = \overline{\xi}_2 - \overline{\xi}_1$, and $\Delta \overline{X}^{cv} = \overline{X}_2^{cv} - \overline{X}_1^{cv}$. Integration of the parameterized total-differential along the direct pathline can then be simplified as presented in Equation 14.

$$\int_0^1 \Delta \overline{X}\, ds \;=\; \int_0^1 \left.\frac{\partial \overline{X}}{\partial \overline{\xi}}(\overline{X}^{cv}(s))\right|_{1\rightarrow 2} \Delta \overline{\xi}\, ds \;+\; \int_0^1 \left.\frac{\partial \overline{X}}{\partial \overline{X}^{cv}}(\overline{\xi}(s))\right|_{1\rightarrow 2} \Delta \overline{X}^{cv}\, ds \tag{14}$$

The parameterized transformation matrices within Equation 14, $\partial \overline{X}(\overline{X}^{cv}(s))/\partial \overline{\xi}$ and $\partial \overline{X}(\overline{\xi}(s))/\partial \overline{X}^{cv}$, are formed by substituting $\overline{\xi}(s)$ and $\overline{X}^{cv}(s)$ from Equation 12 into Equations 4 and 8. These interpolation derivatives are linear with respect the parameterization variable, and include constant particle end-state coordinates: $\overline{\xi}_1$, $\overline{\xi}_2$, $\overline{X}_1^{cv}$ and $\overline{X}_2^{cv}$. Solution of Equation 14 is then straightforward, and many expansions may be obtained. The three discrete-expansions most easily obtained using the direct integration pathline are presented in Equation 15.

$$
\begin{aligned}
\Delta\bar{X} &= \frac{\partial \bar{X}}{\partial \bar{\xi}}(\hat{\bar{X}}^{cv})\,\Delta\bar{\xi} + \frac{\partial \bar{X}}{\partial \bar{X}^{cv}}(\hat{\bar{\xi}})\,\Delta\bar{X}^{cv} \\
\Delta\bar{X} &= \frac{\partial \bar{X}}{\partial \bar{\xi}}(\bar{X}_1^{cv})\,\Delta\bar{\xi} + \frac{\partial \bar{X}}{\partial \bar{\xi}}(\Delta\bar{X}^{cv})\,\Delta\bar{\xi} + \frac{\partial \bar{X}}{\partial \bar{X}^{cv}}(\bar{\xi}_1)\,\Delta\bar{X}^{cv} \\
\Delta\bar{X} &= \frac{\partial \bar{X}}{\partial \bar{\xi}}(\bar{X}_2^{cv})\,\Delta\bar{\xi} - \frac{\partial \bar{X}}{\partial \bar{\xi}}(\Delta\bar{X}^{cv})\,\Delta\bar{\xi} + \frac{\partial \bar{X}}{\partial \bar{X}^{cv}}(\bar{\xi}_2)\,\Delta\bar{X}^{cv}
\end{aligned}
\tag{15}
$$

The linear discrete-expansions within Equation 15 are similar to a Taylor's series of a linear function: they are combinations of scaled derivatives and have a limited number of terms; for linear interpolation, only first-order derivatives are non-zero. Arguments for the transformation matrices are either particle end-state coordinates or the averages: $\hat{\bar{\xi}} = (\bar{\xi}_1 + \bar{\xi}_2)/2$ and $\hat{\bar{X}}^{cv} = (\bar{X}_1^{cv} + \bar{X}_2^{cv})/2$. The interpolation derivatives are scaled by finite-difference vectors of the logical-coordinates and cell-vertex coordinates: $\Delta\bar{\xi}$ and $\Delta\bar{X}^{cv}$.

Upper-Step Integration Pathline

The second integration pathline used to solve Equation 11 is comprised of two line-segments between particle States 1 and 2. The first pathline segment is a line of constant $\bar{\xi}$ from State 1 to State A; see Figure 2. State A is a collection of logical-coordinates defined at State 1 and cell-vertex coordinates defined at State 2: $\bar{X}_A = \bar{X}(\bar{\xi}_1, \bar{X}_2^{cv})$. The second pathline segment is a line of constant $\bar{X}^{cv}$ from State A to State 2. These two pathline segments form an upper-step within the $(\bar{\xi}, \bar{X}^{cv})$ plane. The parameterized coordinates are presented in Equations 16 and 17.

$$
\begin{aligned}
\text{State 1} \rightarrow \text{State A} \quad : \quad \bar{X}(s) &= (1-s)\,\bar{X}_1 + (s)\,\bar{X}_A \\
\bar{\xi}(s) &= (1-s)\,\bar{\xi}_1 + (s)\,\bar{\xi}_A \;;\; \bar{\xi}_A = \bar{\xi}_1 \\
&= \bar{\xi}_1 \\
\bar{X}^{cv}(s) &= (1-s)\,\bar{X}_1^{cv} + (s)\,\bar{X}_A^{cv} \;;\; \bar{X}_A^{cv} = \bar{X}_2^{cv} \\
&= (1-s)\,\bar{X}_1^{cv} + (s)\,\bar{X}_2^{cv}
\end{aligned}
\tag{16}
$$

$$
\begin{aligned}
\text{State A} \rightarrow \text{State 2} \quad : \quad \bar{X}(s) &= (1-s)\,\bar{X}_A + (s)\,\bar{X}_2 \\
\bar{\xi}(s) &= (1-s)\,\bar{\xi}_A + (s)\,\bar{\xi}_2 \;;\; \bar{\xi}_A = \bar{\xi}_1 \\
&= (1-s)\,\bar{\xi}_1 + (s)\,\bar{\xi}_2 \\
\bar{X}^{cv}(s) &= (1-s)\,\bar{X}_A^{cv} + (s)\,\bar{X}_2^{cv} \;;\; \bar{X}_A^{cv} = \bar{X}_2^{cv} \\
&= \bar{X}_2^{cv}
\end{aligned}
\tag{17}
$$

The upper-step integration pathline does not constitute cell-based partition of the original, non-parameterized total-differential, Equation 10. Instead, the upper-step pathline is used to integrate the parameterized total-differential, which is not dependent upon cell-based coordinate systems. Integration of the non-parameterized total-differential, Equation 10, can be rewritten to simulate the upper-step integration pathline as presented in Equation 18.

$$\begin{aligned}\int_1^A d\bar{X} + \int_A^2 d\bar{X} &= \int_1^A \frac{\partial \bar{X}}{\partial \bar{\xi}}(\bar{X}^{cv})\, d\bar{\xi} + \int_A^2 \frac{\partial \bar{X}}{\partial \bar{\xi}}(\bar{X}^{cv})\, d\bar{\xi} \\ &+ \int_1^A \frac{\partial \bar{X}}{\partial \bar{X}^{cv}}(\bar{\xi})\, d\bar{X}^{cv} + \int_A^2 \frac{\partial \bar{X}}{\partial \bar{X}^{cv}}(\bar{\xi})\, d\bar{X}^{cv}\end{aligned} \tag{18}$$

Parameterization of Equation 18, the upper-step integration pathline, is represented in Equation 19, where the interpolation derivatives are appropriately labeled.

$$\begin{aligned}&\int_0^1 \frac{\partial \bar{X}(s)}{\partial s}\bigg|_{1\to A} ds + \int_0^1 \frac{\partial \bar{X}(s)}{\partial s}\bigg|_{A\to 2} ds = \\ &+ \int_0^1 \frac{\partial \bar{X}}{\partial \bar{\xi}}(\bar{X}^{cv}(s))\bigg|_{1\to A} \frac{\partial \bar{\xi}(s)}{\partial s}\bigg|_{1\to A} ds + \int_0^1 \frac{\partial \bar{X}}{\partial \bar{\xi}}(\bar{X}^{cv}(s))\bigg|_{A\to 2} \frac{\partial \bar{\xi}(s)}{\partial s}\bigg|_{A\to 2} ds \\ &+ \int_0^1 \frac{\partial \bar{X}}{\partial \bar{X}^{cv}}(\bar{\xi}(s))\bigg|_{1\to A} \frac{\partial \bar{X}^{cv}(s)}{\partial s}\bigg|_{1\to A} ds + \int_0^1 \frac{\partial \bar{X}}{\partial \bar{X}^{cv}}(\bar{\xi}(s))\bigg|_{A\to 2} \frac{\partial \bar{X}^{cv}(s)}{\partial s}\bigg|_{A\to 2} ds\end{aligned} \tag{19}$$

Along each segment of the upper-step integration pathline, one of the coordinate variables is held constant; the derivative of this parameterized coordinate is the null vector. Along the first pathline segment from State 1 to State A, where $\bar{\xi}$ is held constant, $\partial\bar{\xi}(s)/\partial s = 0$ and $\partial\bar{X}^{cv}(s)/\partial s = \Delta\bar{X}^{cv}$. Alternately, along the second pathline segment from State A to State 2, where $\bar{X}^{cv}$ is held constant, $\partial\bar{\xi}(s)/\partial s = \Delta\bar{\xi}$ and $\partial\bar{X}^{cv}(s)/\partial s = 0$. Along the entire upper-step pathline $\partial\bar{X}(s)/\partial s = \Delta\bar{X}$. Integration of the parameterized total-differential along the upper-step pathline can then be simplified as presented in Equation 20.

$$\int_0^1 \Delta\bar{X}\, ds = \int_0^1 \frac{\partial \bar{X}}{\partial \bar{\xi}}(\bar{X}^{cv}(s))\bigg|_{A\to 2} \Delta\bar{\xi}\, ds + \int_0^1 \frac{\partial \bar{X}}{\partial \bar{X}^{cv}}(\bar{\xi}(s))\bigg|_{1\to A} \Delta\bar{X}^{cv}\, ds \tag{20}$$

The parameterized transformation matrices in Equation 20 are formed by substituting $\bar{\xi}(s)$ and $\bar{X}^{cv}(s)$ from Equations 16 and 17 into Equations 4 and 8. Solution of Equation 20 is then straightforward, and many expansions may be obtained. The single discrete-expansion most easily obtained using the upper-step integration pathline is presented in Equation 21.

$$\Delta\bar{X} \;=\; \frac{\partial \bar{X}}{\partial \bar{\xi}}(\bar{X}_2^{cv})\;\Delta\bar{\xi} \;+\; \frac{\partial \bar{X}}{\partial \bar{X}^{cv}}(\bar{\xi}_1)\;\Delta\bar{X}^{cv} \tag{21}$$

The linear discrete-expansion within Equation 21 is a combination of scaled first-order interpolation derivatives. Within Equation 21, the coordinate-transformation matrix, $\partial\bar{X}/\partial\bar{\xi}$, is evaluated with a cell-vertex coordinate vector defined at $\bar{X}_2^{cv}$; the logical-coordinates vary along the pathline segment where $\bar{X}^{cv}$ is fixed at State 2. Similarly, within Equation 21 the geometry-transformation matrix, $\partial\bar{X}/\partial\bar{X}^{cv}$, is evaluated with a logical-coordinate vector defined at $\bar{\xi}_1$; the cell-vertex coordinates vary along the pathline segment where $\bar{\xi}$ is fixed at State 1. Application of this linear discrete-expansion, obtained by integrating along the upper-step pathline, for numerical analysis and localization within particle methods will be discussed and outlined below.

Lower-Step Integration Pathline

The third integration pathline used to solve Equation 11 is similar to the upper-step pathline. This final pathline alternative is also comprised of two line-segments between particle States 1 and 2. The first pathline segment is a line of constant $\bar{X}^{cv}$ from State 1 to State B; see Figure 2. State B is a collection of logical-coordinates defined at State 2 and cell-vertex coordinates defined at State 1: $\bar{X}_B = \bar{X}(\bar{\xi}_2, \bar{X}_1^{cv})$. The second pathline segment is a line of constant $\bar{\xi}$ from State B to State 2. These two pathline segments form a lower-step within the $(\bar{\xi}, \bar{X}^{cv})$ plane. The parameterized coordinates are presented in Equations 22 and 23.

$$\begin{aligned}
\text{State 1} \rightarrow \text{State B} \quad : \quad \bar{X}(s) &= (1-s)\,\bar{X}_1 + (s)\,\bar{X}_B \\
\bar{\xi}(s) &= (1-s)\,\bar{\xi}_1 + (s)\,\bar{\xi}_B \;;\; \bar{\xi}_B = \bar{\xi}_2 \\
&= (1-s)\,\bar{\xi}_1 + (s)\,\bar{\xi}_2 \\
\bar{X}^{cv}(s) &= (1-s)\,\bar{X}_1^{cv} + (s)\,\bar{X}_B^{cv} \;;\; \bar{X}_B^{cv} = \bar{X}_1^{cv} \\
&= \bar{X}_1^{cv}
\end{aligned} \tag{22}$$

$$\begin{aligned}
\text{State B} \rightarrow \text{State 2} \quad : \quad \bar{X}(s) &= (1-s)\,\bar{X}_B + (s)\,\bar{X}_2 \\
\bar{\xi}(s) &= (1-s)\,\bar{\xi}_B + (s)\,\bar{\xi}_2 \;;\; \bar{\xi}_B = \bar{\xi}_2 \\
&= \bar{\xi}_2 \\
\bar{X}^{cv}(s) &= (1-s)\,\bar{X}_B^{cv} + (s)\,\bar{X}_2^{cv} \;;\; \bar{X}_B^{cv} = \bar{X}_1^{cv} \\
&= (1-s)\,\bar{X}_1^{cv} + (s)\,\bar{X}_2^{cv}
\end{aligned} \tag{23}$$

Integration of the non-parameterized total-differential, Equation 10, can be rewritten to simulate the lower-step integration pathline as presented in Equation 24.

$$\int_1^B d\bar{X} + \int_B^2 d\bar{X} = \int_1^B \frac{\partial \bar{X}}{\partial \bar{\xi}}(\bar{X}^{cv})\, d\bar{\xi} + \int_B^2 \frac{\partial \bar{X}}{\partial \bar{\xi}}(\bar{X}^{cv})\, d\bar{\xi} + \int_1^B \frac{\partial \bar{X}}{\partial \bar{X}^{cv}}(\bar{\xi})\, d\bar{X}^{cv} + \int_B^2 \frac{\partial \bar{X}}{\partial \bar{X}^{cv}}(\bar{\xi})\, d\bar{X}^{cv} \tag{24}$$

Parameterization of Equation 24, the lower-step integration pathline, is represented in Equation 25, where the interpolation derivatives are appropriately labeled.

$$\begin{aligned} &\int_0^1 \left.\frac{\partial \bar{X}(s)}{\partial s}\right|_{1\to B} ds + \int_0^1 \left.\frac{\partial \bar{X}(s)}{\partial s}\right|_{B\to 2} ds = \\ &+ \int_0^1 \left.\frac{\partial \bar{X}}{\partial \bar{\xi}}(\bar{X}^{cv}(s))\right|_{1\to B} \left.\frac{\partial \bar{\xi}(s)}{\partial s}\right|_{1\to B} ds + \int_0^1 \left.\frac{\partial \bar{X}}{\partial \bar{\xi}}(\bar{X}^{cv}(s))\right|_{B\to 2} \left.\frac{\partial \bar{\xi}(s)}{\partial s}\right|_{B\to 2} ds \\ &+ \int_0^1 \left.\frac{\partial \bar{X}}{\partial \bar{X}^{cv}}(\bar{\xi}(s))\right|_{1\to B} \left.\frac{\partial \bar{X}^{cv}(s)}{\partial s}\right|_{1\to B} ds + \int_0^1 \left.\frac{\partial \bar{X}}{\partial \bar{X}^{cv}}(\bar{\xi}(s))\right|_{B\to 2} \left.\frac{\partial \bar{X}^{cv}(s)}{\partial s}\right|_{B\to 2} ds \end{aligned} \tag{25}$$

Along each segment of the lower-step integration pathline, one of the coordinate variables is held constant; the derivative of this parameterized coordinate is the null vector. Along the first pathline segment from State 1 to State B, where $\bar{X}^{cv}$ is held constant, $\partial\bar{\xi}(s)/\partial s = \Delta\bar{\xi}$ and $\partial\bar{X}^{cv}(s)/\partial s = 0$. Alternately, along the second pathline segment from State B to State 2, where $\bar{\xi}$ is held constant, $\partial\bar{\xi}(s)/\partial s = 0$ and $\partial\bar{X}^{cv}(s)/\partial s = \Delta\bar{X}^{cv}$. Along the entire lower-step pathline $\partial\bar{X}(s)/\partial s = \Delta\bar{X}$. Integration of the parameterized total-differential along the lower-step pathline can then be simplified as presented in Equation 26.

$$\int_0^1 \Delta\bar{X}\, ds = \int_0^1 \left.\frac{\partial \bar{X}}{\partial \bar{\xi}}(\bar{X}^{cv}(s))\right|_{1\to B} \Delta\bar{\xi}\, ds + \int_0^1 \left.\frac{\partial \bar{X}}{\partial \bar{X}^{cv}}(\bar{\xi}(s))\right|_{B\to 2} \Delta\bar{X}^{cv}\, ds \tag{26}$$

The parameterized transformation matrices in Equation 26 are formed by substituting $\bar{\xi}(s)$ and $\bar{X}^{cv}(s)$ from Equations 22 and 23 into Equations 4 and 8. Solution of Equation 26 is then straightforward, and many expansions may be obtained. The single discrete-expansion most easily obtained using the lower-step integration pathline is presented in Equation 27.

$$\Delta\bar{X} = \frac{\partial \bar{X}}{\partial \bar{\xi}}(\bar{X}_1^{cv})\, \Delta\bar{\xi} + \frac{\partial \bar{X}}{\partial \bar{X}^{cv}}(\bar{\xi}_2)\, \Delta\bar{X}^{cv} \tag{27}$$

The lower-step discrete-expansion, Equation 27, is similar to the upper-step expansion, Equation 21. While the form of these discrete-expansions is identical, their interpolation

derivatives are evaluated at opposite particle end-states; the upper-step and lower-step integration pathlines are mirror images of each other. Within Equation 27, the coordinate-transformation matrix is evaluated at $\overline{X}_1^{cv}$ and the geometry-transformation matrix is evaluated at $\bar{\xi}_2$.

The discrete-expansions in Equations 15, 21, and 27, developed for tetrahedral cells, are identical to the expansions developed for triangles and line-elements; linear interpolation within these two and one-dimensional geometries is a subset of the three-dimensional function. All of these linear discrete-expansions are a simplification of the trilinear [8,9] and bilinear expansions [10,12]; linear interpolation is more simple than a multi-linear function. Furthermore, the upper-step discrete-expansion within Equation 21 is the linear version of the trilinear expansion which was obtained using the finite-difference method. The total-differential and finite-difference methods, therefore, produce identical discrete-expansions for similar interpolation functions.

However, unique discrete-expansion formulations are possible for linear interpolation; the transformation matrices are easily manipulated since they are linear functions of $\bar{\xi}$ and $\overline{X}^{cv}$. Two expansions in Equation 15 include transformation matrices that are evaluated at the identical particle end-state. A second Jacobian matrix, evaluated with $\Delta\overline{X}^{cv}$, also appears in these expansions. The form of these two expansions is not repeated in the multi-linear solutions. Furthermore, these direct-pathline expansions are related to the other linear discrete-expansions; they are equivalent to the upper-step and lower-step expansions in Equations 21 and 27.

Additional discrete-expansions for linear interpolation, beyond the five presented in this report, might be possible using either the total-differential or the finite-difference methods. While the finite-difference method is simple, obtaining an expansion with this technique requires knowledge of the desired solution. In contrast, the integration of a parameterized total-differential is mathematically well founded, and the discrete-expansions are obtained without a-priori knowledge of the solution. Parameterization of the total-differential also transforms the multi-variable integration process, involving each element within $\bar{\xi}$ and $\overline{X}^{cv}$, into a one-dimensional problem with respect to the parameterization variable. The total-differential method, therefore, represents a general solution technique for developing discrete-expansions for interpolation.

Discussion

Particle methods require expansions of interpolation functions for both numerical analyses and logical-coordinate evaluation. Application of the linear discrete-expansions developed herein for these two purposes is beyond the scope of this report. Verification of the new expansions, however, is provided in Appendix A; one of the new discrete-expansions is demonstrated to correctly solve the general problem for two particles located in separate, non-contiguous cells.

Within the following sections, application of linear discrete-expansions for numerical analyses and localization within particle methods is outlined and discussed.

Numerical Analysis

The goal of numerical analysis, an analytical investigation of a computational model, includes establishing the model's mathematical consistency and numerical accuracy. While estimates of these measures are possible, analytical proof is preferred. A model's consistency and accuracy are based upon its leading-order error term, which is obtained by substituting series expansions for all discrete-terms within the model. A Taylor's series, however, is not a valid expansion through coupled multi-linear interpolation functions. Instead, a discrete-expansion is required to complete numerical analyses of computational models that use interpolation.

Numerical analyses of reactive particle methods require the discrete-expansion of a velocity-interpolation function; these methods compute particle trajectories by interpolating from a discrete velocity field: $\overline{V}(\bar{\xi}, \overline{V}^{cv})$. All numerical analyses require that the discrete-expansion must be written relative to a single state, defined here as State 1. Using multi-step integration methods, however, a reactive particle's velocity might be evaluated in a separate computational sub-domain, defined here as State 2. The objective is then to write a discrete-expansion of the velocity-interpolation function from State 1 to State 2: $\overline{V}_2 = \overline{V}_1 + f(\bar{\xi}_1, \overline{V}_1^{cv})$.

Any one of the above discrete-expansions may be used for numerical analysis; each expansion is valid throughout a discretized domain. One obvious choice would be the common discrete-expansion developed using both the finite-difference and total-differential methods. For linear interpolation, the common discrete-expansion, the upper-step pathline expansion originally presented in Equation 21, is repeated in Equation 28 for a velocity-interpolation function.

$$\overline{V}(\bar{\xi}_2, \overline{V}_2^{cv}) = \overline{V}(\bar{\xi}_1, \overline{V}_1^{cv}) + \frac{\partial \overline{V}}{\partial \bar{\xi}}(\overline{V}_2^{cv})\, \Delta\bar{\xi} + \frac{\partial \overline{V}}{\partial \overline{V}^{cv}}(\bar{\xi}_1)\, \Delta\overline{V}^{cv} \qquad (28)$$

For numerical analysis, discrete-expansions must be defined at State 1, but Equation 28 includes an interpolation derivative defined at State 2: $\partial\overline{V}(\overline{V}_2^{cv})/\partial\bar{\xi}$. Recursive application of the discrete-expansion can transform a mixed-state interpolated velocity into a State 1 function: $\overline{V}(\bar{\xi}_1, \overline{V}_2^{cv}) = f(\bar{\xi}_1, \overline{V}_1^{cv})$. This separate single-state velocity-interpolation expansion can be substituted into Equation 28, and the model's numerical analysis may then be completed.

For computational models that use interpolation, discrete-expansions represent a key advancement in the ability to analyze existing models; discrete-expansions provide the capacity to analytically evaluate their mathematical consistency and numerical accuracy. By providing an

analytical description of a model's leading-order error term, discrete-expansions also provide the capacity to develop advanced computational models; the leading-order error term of an existing model may be used to create a new, advanced computational model.

Logical-Coordinate Evaluation

Logical-coordinate evaluation is the transformation of a physical-space position vector into cell-based, logical-space coordinates. Interpolation functions are often used for spatial transformation because they can provide a relationship between physical and logical coordinates. Discrete-expansions represent the mathematical expression that allows interpolation functions to evaluate a particle's logical-coordinates. For linear interpolation, the discrete-expansion originally presented in Equation 21 may be rewritten for this purpose as presented in Equation 29.

$$\frac{\partial \bar{X}}{\partial \bar{\xi}}(\bar{X}_2^{cv})\ \Delta\bar{\xi} \;=\; (\bar{X}_2 - \bar{X}_1) - \frac{\partial \bar{X}}{\partial \bar{X}^{cv}}(\bar{\xi}_1)\ \Delta\bar{X}^{cv} \tag{29}$$

Equation 29 is valid between two particles, States 1 and 2, located in separate, non-contiguous grid cells. For logical-coordinate evaluation, all of the coordinate vectors at State 1 are known: $\bar{X}_1$, $\bar{\xi}_1$ and $\bar{X}_1^{cv}$. In contrast, the only coordinates known at State 2 are the physical-coordinates of the particle: $\bar{X}_2$. The cell-searching portion of the localization algorithm does, however, provide an estimate of the cell-vertex coordinates at State 2: $\bar{X}_2^{cv}$. The only unknown in Equation 29, therefore, is the logical-coordinate vector at State 2, $\bar{\xi}_2$, which is the desired solution embedded within the finite-difference vector $\Delta\bar{\xi} = \bar{\xi}_2 - \bar{\xi}_1$.

Equation 29 is defined between two *fixed* particles. State 2 is *absolutely* fixed, invariant throughout the localization problem, by the particle's physical-coordinates, $\bar{X}_2$. In contrast, State 1 is *arbitrarily* fixed; its position is constrained only by the requirement that $\bar{X}_1 = \bar{X}(\bar{\xi}_1, \bar{X}_1^{cv})$. Bound position vectors may then be selected for use in Equation 29 that guarantees an algorithmically robust method. Solution of Equation 29 is also computationally efficient; all of the interpolation derivatives are constant and only require a single evaluation. In contrast to the multi-linear discrete-expansions, only a single solution of Equation 29 is required for logical-coordinate evaluation since elements of $\bar{\xi}_2$ only appear within $\Delta\bar{\xi}$. Finally, existing evaluation methods, which are based on Taylor's series, may be obtained from Equation 29 if $\bar{X}_2^{cv} = \bar{X}_1^{cv}$.

Summary

Five new discrete-expansions were developed for linear interpolation defined within three-dimensional tetrahedral cell geometries. Discrete-expansions are similar to multi-variable expansions, but unlike a Taylor's series, they are valid throughout a discretized domain; they

account for interpolation discontinuities across cell boundaries. The new expansions were developed by parametrically integrating the interpolation function's total-differential between two particles located in separate, non-contiguous cells. The three-dimensional linear discrete-expansions are identical to those developed for two-dimensional triangles and one-dimensional line-elements. The linear expansions are also a simplification of multi-linear discrete-expansions, but the linear expansions exhibit unique formulations and utilization characteristics.

For any computational model that uses interpolation, discrete-expansions represent a key advancement; they provide the capacity to analytically define a model's leading-order error term and, therefore, establish the mathematical consistency and numerical accuracy of existing models. Discrete-expansions also provide the capacity to develop advanced computational models; the leading-order error term of an existing model may be used to a create a new, more accurate model. Furthermore, the use of discrete-expansions for logical-coordinate evaluation provides an algorithmically robust and computationally efficient particle localization method. Finally, linear discrete-expansions may be simplified to obtain the existing logical-coordinate evaluation methods, which are based upon a truncated, single-variable Taylor's series expansion.

Acknowledgement

This work was sponsored by the Accelerated Strategic Computing Initiative Program at the Los Alamos National Laboratory. Thanks to Forrest B. Brown, John H. Hall and Stephen R. Lee of the Blanca Project for their support of this investigation. Much thanks to James R. Kamm and Gary L. Sandine of the Applied Physics Division for assistance in this research.

References

1) Allievi, A. and Bermejo, R., “A Generalized Particle-Search Algorithm for Arbitrary Grids,” *Journal of Computational Physics*, Vol. 132, pp. 157-166, 1997.

2) Lohner, R., “Robust, Vectorized Search Algorithms for Interpolation on Unstructured Grids,” *Journal of Computational Physics*, Vol. 118, pp. 380-387, 1995.

3) Westerman, T., “Localization Schemes in 2D Boundary-Fitted Grids,” *Journal of Computational Physics*, Vol. 101, pp. 307-313, 1992.

4) Lohner, R. and Ambrosiano, J. “A Vectorized Particle Tracer for Unstructured Grids,” *Journal of Computational Physics*, Vol. 91, pp. 22-31, 1990.

5) Wilson, T. L., “LINTERP: A Numerical Algorithm for Interpolating Quadrilateral and Hexahedral Meshes,” Los Alamos National Laboratory Report LA-11902-MS, 1990.

6) Brackbill, J. U. and Ruppel, H. M., “FLIP: A Method for Adaptively Zoned, Particle-in-Cell Calculations of Fluid Flows in Two Dimensions,” *Journal of Computational Physics*, Vol. 65, pp. 314-343, 1986.

7) Pracht, W. E. and Brackbill, J. U., “BAAL: A Code for Calculating Three-Dimensional Fluid Flows at All Speeds with an Eulerian-Lagrangian Computing Mesh,” Los Alamos National Laboratory Report LA-6342, 1976.

8) Brock, J. S., “A Finite-Difference Logical-Coordinate Evaluation Method For Particle Localization,” *Progress of Theoretical Physics*, Sup. 138, pp. 40-42, 2000. (Los Alamos National Laboratory Report LA-UR-99-6493, 1999.)

9) Brock, J. S., “A New Logical-Coordinate Evaluation Method For Particle Localization,” Los Alamos National Laboratory Report LA-UR-99-5355, 1999.

10) Wiseman, J. R. and Brock, J. S., “Integrating Interpolation Functions Across Triangular and Quadrilateral Cell Boundaries,” Los Alamos National Laboratory Report LA-UR-00-3331, 2000.

11) Wiseman, J. R. and Brock, J. S., “Integrating a Linear Interpolation Function Across Triangular Cell Boundaries,” Los Alamos National Laboratory Report LA-UR-00-3330, 2000.

12) Brock, J. S., “Integrating a Bilinear Interpolation Function Across Quadrilateral Cell Boundaries,” Los Alamos National Laboratory Report LA-UR-00-3329, 2000.

Appendix A: Test Problem

The purpose of this appendix is to verify that the five discrete-expansions presented in this report, developed for three-dimensional linear interpolation, are valid across tetrahedral cell boundaries. The following verification has been performed for each expansion in Equations 15, 21, and 27. Within this appendix, however, only one discrete-expansion is used to solve the general problem of two particles located in separate, non-contiguous grid cells. The expansion selected for this demonstration, originally presented in Equation 15, is repeated in Equation A-1.

$$\Delta\bar{X} = \frac{\partial\bar{X}}{\partial\bar{\xi}}(\hat{\bar{X}}^{cv})\,\Delta\bar{\xi} + \frac{\partial\bar{X}}{\partial\bar{X}^{cv}}(\hat{\bar{\xi}})\,\Delta\bar{X}^{cv} \tag{A-1}$$

A particle's state is comprised of a set of physical-coordinates, $\bar{X} = (x, y, z)^T$, logical-coordinates, $\bar{\xi} = (\xi, \eta, \zeta)^T$, and cell-vertex coordinates, $\bar{X}^{cv} = ({}^0\bar{X}, {}^1\bar{X}, {}^2\bar{X}, {}^3\bar{X})^T$. The only restriction on particle states is that they must form a consistent set of coordinates as described by the interpolation function: $\bar{X} = \bar{X}(\bar{\xi}, \bar{X}^{cv})$. For this demonstration, the two particle states, State 1 and State 2, are defined in Equations A-2 and A-3.

$$\begin{aligned} \text{State 1} \quad : \quad \bar{X}_1 &= (0.2, 0.8, 0.3)^T \\ \bar{\xi}_1 &= (0.2, 0.4, 0.1)^T \\ \bar{X}_1^{cv} &= (0, 0, 0, 1, 0, 0, 0, 2, 0, 0, 0, 3)^T \end{aligned} \tag{A-2}$$

$$\begin{aligned} \text{State 2} \quad : \quad \bar{X}_2 &= (4.9, 4.4, 3.5)^T \\ \bar{\xi}_2 &= (0.1, 0.3, 0.5)^T \\ \bar{X}_2^{cv} &= (5, 5, 2, 4, 5, 2, 5, 3, 2, 5, 5, 5)^T \end{aligned} \tag{A-3}$$

The discrete-expansion in Equation A-1 includes two first-order interpolation derivatives, $\partial\bar{X}/\partial\bar{\xi}$ and $\partial\bar{X}/\partial\bar{X}^{cv}$. Both transformation matrices are evaluated with average logical-coordinates and average cell-vertex coordinates: $\hat{\bar{\xi}} = (\bar{\xi}_1 + \bar{\xi}_2)/2$ and $\hat{\bar{X}}^{cv} = (\bar{X}_1^{cv} + \bar{X}_2^{cv})/2$. For this demonstration, these average coordinate vectors are presented in Equation A-4.

$$\begin{aligned} \text{State Average} \quad : \quad \hat{\bar{\xi}} &= (\hat{\xi}, \hat{\eta}, \hat{\zeta})^T \\ &= (0.15, 0.35, 0.30)^T \\ \hat{\bar{X}}^{cv} &= ({}^0\hat{x}, {}^0\hat{y}, {}^0\hat{z}, {}^1\hat{x}, {}^1\hat{y}, {}^1\hat{z}, {}^2\hat{x}, {}^2\hat{y}, {}^2\hat{z}, {}^3\hat{x}, {}^3\hat{y}, {}^3\hat{z})^T \\ &= (2.5, 2.5, 1, 2.5, 2.5, 1, 2.5, 2.5, 1, 2.5, 2.5, 4)^T \end{aligned} \tag{A-4}$$

The first-order interpolation derivatives in Equation A-1 are scaled by the finite-difference vectors $\Delta\bar{\xi}$ and $\Delta\bar{X}^{cv} = (\Delta^0\bar{X}, \Delta^1\bar{X}, \Delta^2\bar{X}, \Delta^3\bar{X})^T$. These vectors are presented in Equation A-5.

$$\begin{aligned} \text{State Delta} \quad : \quad \Delta\bar{X} &= (\Delta x, \Delta y, \Delta z)^T = (4.7, 3.6, 3.2)^T \\ \Delta\bar{\xi} &= (\Delta\xi, \Delta\eta, \Delta\zeta)^T = (-0.1, -0.1, 0.4)^T \\ \Delta\bar{X}^{cv} &= (\Delta^0 x, \Delta^0 y, \Delta^0 z, \Delta^1 x, \Delta^1 y, \Delta^1 z, \Delta^2 x, \Delta^2 y, \Delta^2 z, \Delta^3 x, \Delta^3 y, \Delta^3 z)^T \\ &= (5, 5, 2, 3, 5, 2, 5, 1, 2, 5, 5, 2)^T \end{aligned} \tag{A-5}$$

The Jacobian matrix in Equation A-1, $\partial\bar{X}/\partial\bar{\xi}$, was presented in Equation 3 for three-dimensional coordinate transformations. The elements of this matrix were defined in Equation 4. The geometry-transformation matrix, $\partial\bar{X}/\partial\bar{X}^{cv}$, was presented in Equation 5. The product of this matrix and the finite-difference vector $\Delta\bar{X}^{cv}$ is presented in Equation A-6.

$$\frac{\partial\bar{X}}{\partial\bar{X}^{cv}}\,\Delta\bar{X}^{cv} = \frac{\partial\bar{X}}{\partial^0\bar{X}}\,\Delta^0\bar{X} + \frac{\partial\bar{X}}{\partial^1\bar{X}}\,\Delta^1\bar{X} + \frac{\partial\bar{X}}{\partial^2\bar{X}}\,\Delta^2\bar{X} + \frac{\partial\bar{X}}{\partial^3\bar{X}}\,\Delta^3\bar{X} \tag{A-6}$$

As previously noted, the non-square geometry-transformation matrix may be partitioned into diagonal sub-matrices: $\partial\bar{X}/\partial^v\bar{X}$ where $v = 0, 1, 2, 3$. The non-zero elements of each sub-matrix are identical; they are one of the four linear interpolation basis functions. Each sub-matrix may then be defined as an identity matrix scaled by a basis function. The matrix-vector product in Equation A-6 may then be simplified as presented in Equation A-7.

$$\begin{aligned} \frac{\partial\bar{X}}{\partial\bar{X}^{cv}}\,\Delta\bar{X}^{cv} = {} & (1 - \xi - \eta - \zeta)\,\Delta^0\bar{X} \\ & + (\quad \xi \quad)\,\Delta^1\bar{X} \\ & + (\quad \eta \quad)\,\Delta^2\bar{X} \\ & + (\quad \zeta \quad)\,\Delta^3\bar{X} \end{aligned} \tag{A-7}$$

The derivatives and coordinate finite-difference vectors for linear interpolation, required by each discrete-expansion presented in this report, have been defined analytically. The interpolation derivatives were presented as a function of the vectors $\bar{\xi}$ and $\bar{X}^{cv}$. In contrast, the interpolation derivatives in Equation A-1 are evaluated with the average vectors $\hat{\bar{\xi}}$ and $\hat{\bar{X}}^{cv}$. These average coordinate vectors were defined in Equation A-4. The coordinate finite-difference vectors $\Delta\bar{\xi}$ and $\Delta\bar{X}^{cv}$ were defined in Equation A-5. The algebraic form of Equation A-1, including matrices, vectors, scalars, and their products, is presented in Equation A-8.

$$\Delta\bar{X} = \frac{\partial \bar{X}}{\partial \bar{\xi}}(\hat{\bar{X}}^{cv})\,\Delta\bar{\xi} + \frac{\partial \bar{X}}{\partial \bar{X}^{cv}}(\hat{\bar{\xi}})\,\Delta\bar{X}^{cv}$$

$$= \begin{bmatrix} 0 & 0 & 0 \\ 0 & 0 & 0 \\ 0 & 0 & 3 \end{bmatrix} \begin{Bmatrix} -0.1 \\ -0.1 \\ 0.4 \end{Bmatrix} + (0.2)\begin{Bmatrix} 5 \\ 5 \\ 2 \end{Bmatrix} + (0.15)\begin{Bmatrix} 3 \\ 5 \\ 2 \end{Bmatrix} + (0.35)\begin{Bmatrix} 5 \\ 1 \\ 2 \end{Bmatrix} + (0.3)\begin{Bmatrix} 5 \\ 5 \\ 2 \end{Bmatrix} \qquad \text{(A-8)}$$

$$= (4.7, 3.6, 3.2)^{T}$$

Equation A-8 correctly predicts the change in particle physical-coordinates between State 1 and State 2: $\Delta\bar{X} = (4.7, 3.6, 3.2)^{T}$. Any symmetry or structure exhibited in Equation A-8 is not an inherent feature of discrete-expansions. Instead, these features are an artifact of the test problem. This test problem clearly demonstrates that the five discrete-expansions presented in this report are valid expansions for linear interpolation across tetrahedral cell boundaries.

Figures

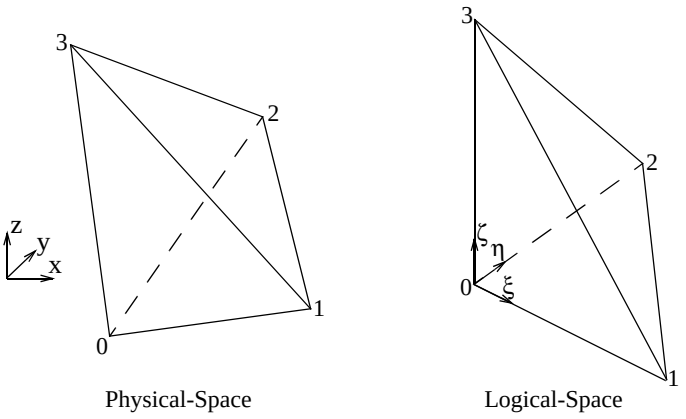

Figure 1: Coordinate Transformation

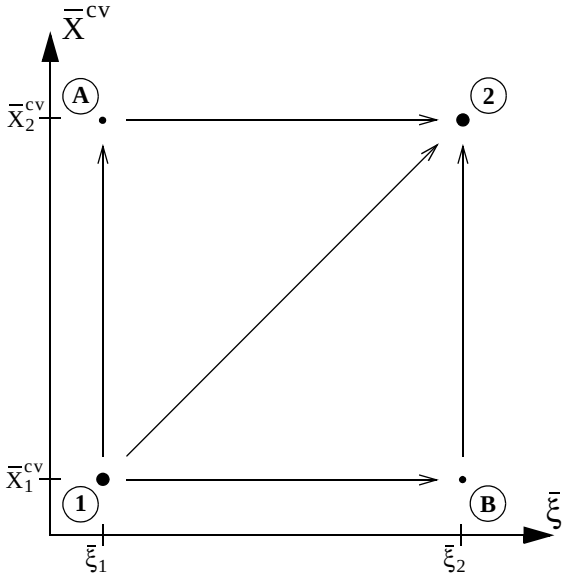

Figure 2: Integration Pathlines